Molecular Vision 2020; 26:97-105 <http://www.molvis.org/molvis/v26/97>
Received 17 October 2019 | Accepted 1 March 2020 | Published 3 March 2020

A simple and efficient method for generating human retinal organoids

Florian Regent, Holly Y. Chen, Ryan A. Kelley, Zepeng Qu, Anand Swaroop, Tiansen Li

Neurobiology, Neurodegeneration & Repair Laboratory, National Eye Institute, National Institutes of Health, Bethesda, MD

Purpose: Retinal organoids (ROs) derived from human pluripotent stem cells largely recapitulate key features of in vivo retinal development, thus permitting the study of retinogenesis, disease modeling, and therapeutic development. However, the complexities of current protocols limit the use of this in vitro system in applications requiring large-scale production of organoids. Currently, widely used methods require the isolation of presumed optic vesicle-like structures from adherent cultures by dissection, a labor-intensive and time-consuming step that involves extensive practice and training.

Method: We report a simple and efficient method for generating ROs by scraping the entire adherent culture and growing the resulting cell aggregates in a free-floating condition.

Results: Within 1 to 7 days following the procedure, emerging morphologically well-defined optic vesicles can be identified and harvested with ease. The transition from two-dimensional (2D) to 3D culture condition favored the formation of ROs from areas devoid of typical optic vesicle-like structures, thus increasing the RO yield. Moreover, ROs generated by this approach were more often associated with the pigment epithelium.

Conclusions: This improved, robust, and efficient protocol should facilitate large-scale differentiation of pluripotent stem cells into retinal organoids in support of human disease modeling and therapy development.

Hereditary retinal degenerative diseases, such as retinitis pigmentosa and Leber congenital amaurosis, are clinically and genetically heterogeneous conditions that lead to progressive loss of vision [1,2]. Currently, few therapeutic options are available, at least in part, due to the physiologic differences between human and animal models and the lack of in vitro systems to efficiently evaluate therapies. With advances in three-dimensional (3D) culture systems, human pluripotent stem cells (hPSCs) can be differentiated into retinal organoids (ROs). These organoids broadly mimic in vivo retinogenesis and retinal morphology, with appropriate apical-basal polarity and time-dependent self-patterning of major cell types into a laminated structure [3-6]. Subsequent improvements of differentiation protocols generated ROs with rudimentary outer segment-like structures and light responses, suggesting at least partially functional maturation of photoreceptors in culture [7-11].

ROs carrying retinal disease-causing mutations could potentially recapitulate disease progression in vitro and facilitate the development of effective treatments [12]. However, despite initial successful attempts at modeling inherited retinal dystrophies [13-16], the high degree of complexity and relatively low yield in current protocols remain significant technical challenges, particularly for inexperienced personnel. Currently widely used differentiation protocols require labor-intensive and time-consuming dissection of optic vesicle (OV)-like domains after such structures have emerged in adherent cultures [7,17,18], thus hindering applications that require large-scale production of ROs, such as biochemical studies and high-throughput drug screening. Furthermore, the efficiency of this step can drastically vary depending on dissection skills and the ability to correctly identify prospective OV domains, which are not always morphologically well defined in adherent cultures. In addition, organoids generated from dissection often lack RPE domains, which are normally concomitantly generated, positionally contiguous with the neural retina (NR), and play an important role in retinal differentiation and photoreceptor maintenance [19].

We report a significant yet simple modification of the conventional methods for generating retinal organoids from pluripotent stem cells, which is more efficient, robust, and convenient. In lieu of dissecting out prospective OV domains, the adherent culture is scraped off entirely and cultured in a free-floating condition. OVs with classical appearance and clear lamination emerged within 1 day. The OVs are easy to identify and require little effort in harvesting. We evaluated this method using one human embryonic stem cell (hESC) line and five human induced pluripotent stem cell (hiPSC) lines and obtained up to a fivefold higher yield of ROs. These organoids are more consistently associated with an RPE-like domain, and thus, better mimic human retina morphogenesis.

Correspondence to: Tiansen Li, Building 6, Room 337, 6 Center Drive, Bethesda, MD 20892; Phone: 301-443-2833; email: Tiansen.Li@nih.gov

METHODS

Generation and maintenance of hPSCs: The CRX-GFP hESC line (a derivative of H9) was generated and characterized as described in our previous publication [20]. The hiPSC lines PEN8E, 901, 902, 1C, and 2D were reprogrammed from skin biopsies using integration-free Sendai virus carrying the four Yamanaka factors, as previously described [12]. Characterization of PEN8E, 1C, and 2D has been reported [13]. Pluripotency of 901 and 902 was confirmed with immunostaining of multiple pluripotency markers SSEA4, OCT4, TRA-1-60, and NANOG (data not shown). All hPSC lines were maintained in growth factor-reduced (GFR) or hESC-qualified Matrigel (Corning, NY)-coated plates using either Essential 8 (E8; ThermoFisher Scientific, Waltham, MA) or mTeSR1 medium (StemCell Technologies, Inc., Vancouver, Canada). hPSCs were passaged at 60% to 80% confluency using the EDTA-based protocol.

Embryoid body formation and OV induction in adherent cultures: hPSCs were induced to form OVs as previously described [7,11]. Briefly, to start differentiation, hPSCs from one well of a six-well plate were dissociated into small clumps using 0.5 mM EDTA/PBS (1X, 2.7 mM KCl, 1.5 mM KH_2PO_4, 137.9 mM NaCl, 8.1 mM Na_2HPO_4-$7H_2O$, pH 7.4; Corning, NY), resuspended in either E8 or mTeSR1 medium supplemented with 10 µM Y-27632 (Tocris, Bristol, UK), and transferred into one 100-mm polyHEMA (Sigma, St. Louis, MO)-coated Petri dish for embryoid body (EB) formation. Neural induction medium (NIM) composed of Dulbecco's Modified Eagle Medium (DMEM)/F-12 (1:1; ThermoFisher Scientific, Waltham, MA) supplemented with 1% N2 supplement (ThermoFisher Scientific), 1X MEM non-essential amino acids (NEAAs; Sigma, St. Louis, MO), and 2 µg/ml heparin (Sigma) was supplied to the culture at a ratio of 3:1 and 1:1 at differentiation day (D) 1 and 2, respectively. At D3, the media were switched to 100% NIM. EBs from one 100-mm Petri dish were plated onto a 60-mm Petri dish coated with BD GFR Matrigel at D7 and cultured in NIM for 9 additional days, with the media changed every 2–3 days. At D16, the media were completely switched to 3:1 retinal induction medium (3:1 RIM) composed of DMEM/F-12 (3:1) supplemented with 2% B_{27} supplement without vitamin A (ThermoFisher Scientific), 1% antibiotic-antimycotic solution (ThermoFisher Scientific), 1% GlutaMAX (ThermoFisher Scientific), and 1X NEAA (Sigma). The media were changed every 2–3 days until OV-like structures appeared, which usually emerged between D20 and D30 (Figure 1A).

Generation and maintenance of ROs: Adherent cells from one 60-mm Petri dish were scraped off using a cell scraper (Corning, NY) into small clumps (<5 mm^2) between D20 and D30. The resulting clumps were transferred to two polyHEMA-coated 100-mm Petri dishes and maintained in free-floating cultures in 3:1 RIM supplemented with 20 ng/ml insulin-like growth factor 1 (IGF-1; ThermoFisher Scientific). A full media change was performed the next day. Well-formed singlet or doublet optic vesicles can be harvested with a wide-bore pipette. Bunched optic vesicles in a large mass were dissected with a pair of 30 gauge/0.5 inch hypodermic needles fitted to 1 ml syringes using a scissoring motion under a stereomicroscope and transferred to polyHEMA-coated culture dishes.

Starting from D35, 3:1 RIM was supplemented with 20 ng/ml IGF-1, 10% fetal bovine serum (FBS; ThermoFisher Scientific), and 1 mM Taurine (Sigma). From D63 onward, 3:1 RIM was supplemented with 1 µM 9-*cis* retinal, which subsequently decreased to 0.5 µM starting from D91. From D91 until the end of differentiation, 1% N2 supplement (ThermoFisher Scientific) was used instead of B27 supplement without vitamin A. The media were half-changed every 2–3 days until D200, with 9-*cis* retinal and IGF-1 freshly added to the media under dim light environment.

Immunofluorescence: hPSC-derived ROs were collected at different time points and fixed in 2% paraformaldehyde (FD NeuroTechnologies, Columbia, MD) for 1 h at room temperature. ROs were then cryoprotected using a sucrose gradient (15–30%) and embedded in M1 embedding matrix (Thermo Scientific) before sectioning. Ten-micron sections were obtained using Leica Biosystems Cryostat (Buffalo Grove, IL) at −14 °C. Sections were dried on Superfrost Plus Microscope slides (Fisher Scientific, Hampton, NH) and stored at −20 °C until use. For immunostaining, after 30-min incubation in blocking solution (PBS with 10% donkey serum and 0.1% Triton) at room temperature, the sections were incubated with primary antibodies overnight at 4 °C (antibody information and dilution are listed in Appendix 1). After three 10-min washes in PBS, appropriate Alexa Fluor-conjugated secondary antibodies and 4′,6-diamidino-2-phenylindole (DAPI; Invitrogen, Carlsbad, CA) were added for 1 h at room temperature.

Image acquisition and analysis: For bright-field images, samples were visualized and imaged using an EVOS XL Core Cell Imaging System (ThermoFisher Scientific). Fluorescence images were acquired with an LSM-700 or LSM-880 confocal microscope (Zeiss, Oberkochen, Germany) with Zen software. Images were exported, analyzed, and processed with Fiji and Photoshop CC 2019 software.

Statistical analysis: The number of ROs (with or without RPE domains) in three independent differentiation batches were quantified based on morphological criteria (presence

of a phase-bright neuroepithelial outer rim for the NR and the presence of pigmentation for RPE cells). Comparisons between the dissection and scraping methods were performed using the unpaired *t* test, and a p value of less than 0.05 was considered statistically significant.

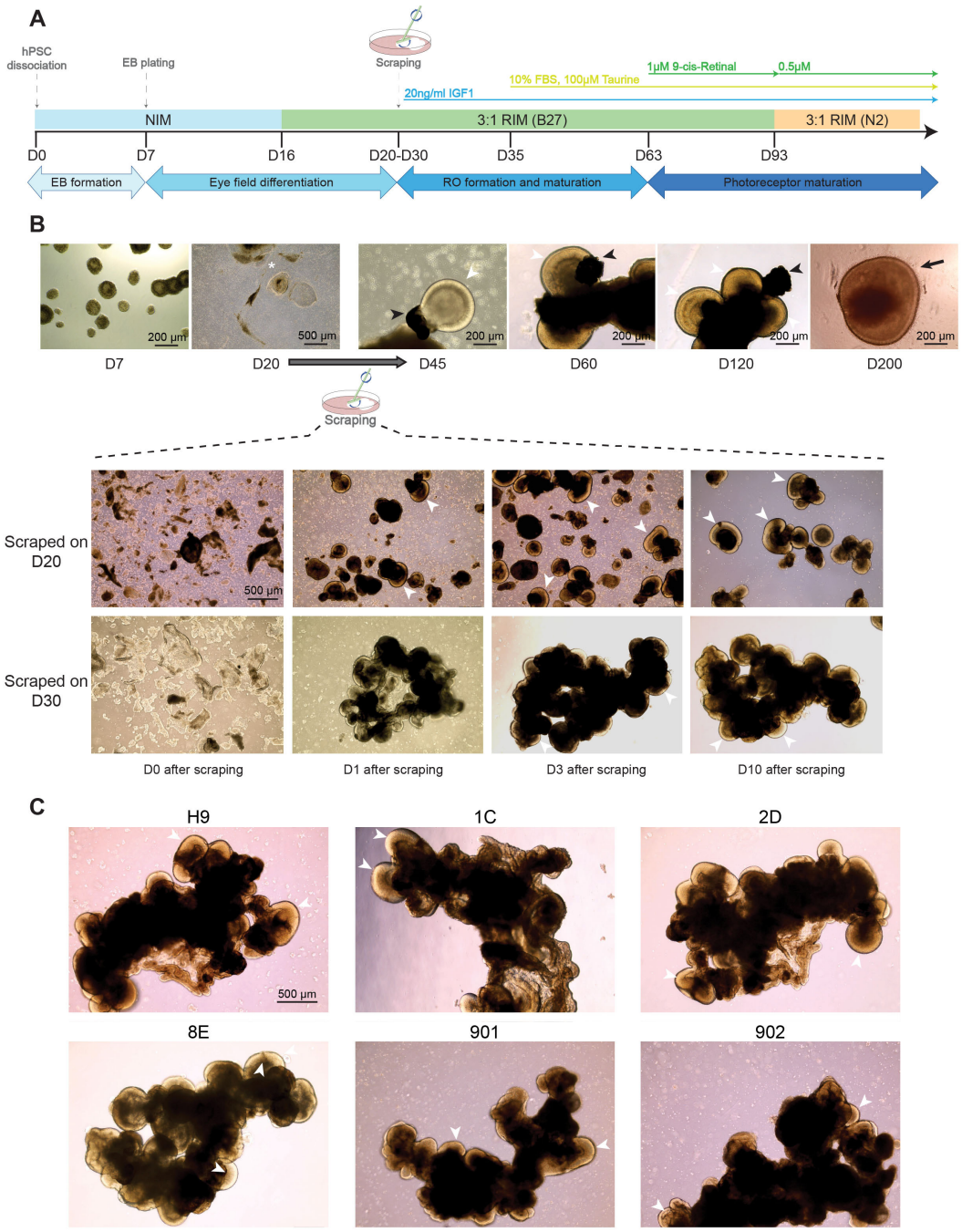

Figure 1. Description of the scraping protocol for differentiating retinal organoids. **A**: Schematic representation of the scraping differentiation protocol used in this study. hPSCs: human pluripotent stem cells; EBs: embryoid bodies; ROs: retinal organoids; NIM: neural induction medium; RIM: retinal induction medium; IGF1: insulin-like growth factor 1. **B**: Representative bright-field images of EBs, cell clumps generated by the scraping method, and differentiating organoids (from D30 to D200). **C**: Representative bright-field images of differentiating ROs 10 days after scraping from hESC line H9 and hiPSC lines 1C, 2D, 8E, 901, and 902. White asterisks: optic vesicle-like structures; white arrowheads: neural retina; black arrowheads: pigmented epithelium domains; black arrow: presumptive photoreceptor cilia.

RESULTS

The scraping method for generating ROs: Retinal differentiation was initiated as previously described [7,11], by aggregating dissociated hPSCs to form EBs and plating them on Matrigel-coated dishes to induce the formation of OV-like domains (Figure 1A). At approximately D20 (counting the first day of EB formation as D0), adherent cells were completely lifted using a cell scraper and dispersed into small pieces and clumps, which were then cultured in free-floating conditions. As short as 24 h after scraping, we consistently observed efficient formation of a high number of ROs in six different hPSC lines, as shown by a phase-bright neuroepithelial outer rim (Figure 1B,C). Depending on the clump size after scraping, formation of individual ROs (Figure 1B, upper row) or bunched ROs (Figure 1B, lower row) was observed. In both cases, ROs were able to differentiate comparably in size and morphology, suggesting that the surrounding tissues in bunched structures did not impair RO growth and differentiation. Given that smaller clumps (<5 mm^2) yielded mostly singlet or doublet OVs that can be cultured to maturity with no need for dissection, they are preferred over the larger bunched ones.

NR in ROs generated by the scraping method: To compare RO production efficiency between the dissection and scraping methods, we quantified the number of ROs generated by both methods at D60–120 using four different cell lines (Figure 2A). Despite variation between cell lines in differentiation efficiency [21], a significant (2.5- to 4.6-fold) increase in RO production was reproducibly obtained by the scraping method compared to dissection. Notably, we were able to obtain OVs by lifting areas “depleted” of OV-like domains after dissection by experienced operators (data not shown), providing a potential explanation for the better yield of the scraping method.

We then assessed whether the ROs produced using the scraping method differentiated in a comparable manner with the dissected ones, by evaluating the biogenesis of major retinal cell types using immunohistochemistry (Figure 2B). Retinal ganglion cells (RGCs) and horizontal cells are the two earliest-born cell types in the human retina. As early as D60, an abundance of RGCs (BRN3A positive) was evident in the innermost layer of the dissected and scraped ROs. However, few BRN3A-positive cells were observed at D200 in ROs generated by both methods, which is consistent with previous studies [11]. Horizontal or amacrine cells (CALB positive) were observed at D60 and D200, regardless of the method used. In ROs obtained with both methods, retinal progenitor marker CHX10 initially expanded to the whole neuroblastic layer at D60 and was subsequently restricted to bipolar cells in the inner nuclear layer at D200, mimicking the in vivo expression pattern. Rod bipolar cells were also shown by PKCα staining in both conditions. Consistent with in vivo retinal development, late-born Müller glial cells were not detected at D60, as shown by the absence of CRALBP staining, but were found expanding in the inner nuclear layers and forming the outer limiting membrane at D200, as the ROs became more mature. Finally, no significant differences were found in photoreceptor development between the dissected and scraped ROs. Regardless of the method used, relatively weak expression of photoreceptor progenitor cell marker RCVRN was observed at D60, suggesting the start of photoreceptor cell fate specification. The robust RCVRN staining at D200, together with the development of outer segment-like structures shown by the staining of rhodopsin and cone opsins (L/M- and S-opsin), indicate the partial maturation of rod and cone photoreceptors in ROs generated by both methods. As shown by ciliary marker ARL13B and basal body marker PCNT, photoreceptor cilia and basal bodies at D200 were correctly aligned at the apical side of the retinal organoids (Figure 2C). Taken together, these results confirmed that ROs obtained with the scraping method displayed similar morphology to those obtained with dissection and recapitulated the temporal development of major retinal cell types in vivo.

Cogeneration of pigment epithelium and NR domains: Additionally, we noted a higher proportion of ROs associated with one or more pigmented domains using the scraping method compared to the dissection. For the four cell lines evaluated, a significantly higher proportion of organoids were found to contain pigmented cells using the scraping method (22.3% to 35.1% by dissection versus 77.2% to 82.6% by scraping, Figure 3A). We then examined the identity of these pigmented cells by assessing the expression of RPE-specific markers with immunostaining (Figure 3B). As expected, cells localized in pigmented domains formed a monolayered epithelium and expressed the pigmentation marker MITF and PMEL17. Moreover, these cells expressed, specifically at their apical membrane, the microvilli-associated proteins EZRIN and MERTK. The latter is a tyrosine kinase receptor involved in phagocytosis of the shed outer segment, confirming their RPE identity and at least partial maturation of these cells as early as D60. In contrast, pigmented domains were less frequently detected in dissected ROs. We also noticed the presence of a distinct subgroup of cells, at the junction between the RPE and NR domains, that coexpressed the ciliary epithelium marker AQP-1 and CHX10 but not the RPE marker MITF. This could indicate the presence of a ciliary margin zone as previously described in human ROs [22] (Figure 3C,D).

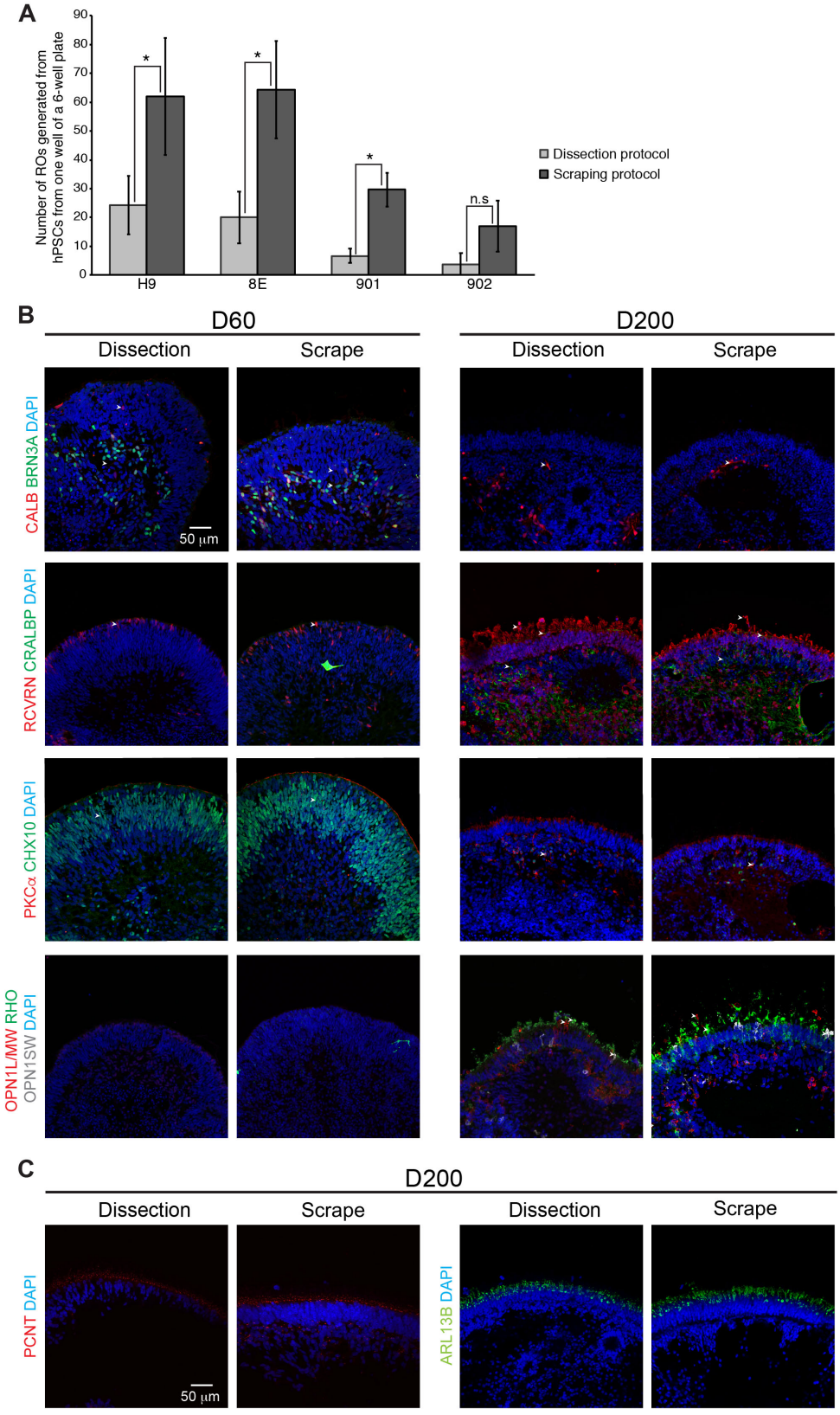

Figure 2. The scraping method improves the yield of ROs with morphology similar to those obtained with dissection. **A**: Quantification of the number of retinal organoids (ROs) produced by the scraping and dissection methods, using human pluripotent stem cells (hPSCs) from one well of a six-well plate. The bar charts summarized data from three independent experiments using four different hPSC lines and presented as mean ± standard deviation. *p<0.05; n.s., non-significant. **B**: Immunohistochemistry analysis of H9 human embryonic stem cell (hESC)-derived ROs using antibodies against markers for retinal ganglion cells (BRN3A, green), horizonal or amacrine cells (CALB, red), photoreceptor progenitor cells (RCVRN, red), Müller glia (CRALBP, green), retinal progenitor cells or bipolar cells (CHX10, green), rod bipolar cells (PKCα, red) and photoreceptors (RHO, green), S-cones (OPN1SW, yellow), and L/M-cones (OPNL/MW, red). **C**: Ciliary markers showing the basal bodies (PCTN, red, left panel) and the cilia (ARL13B, green, right panel) of photoreceptors. Nuclei were stained with 4′,6-diamidino-2-phenylindole (DAPI, blue). Arrowheads indicate relevant staining of each marker.

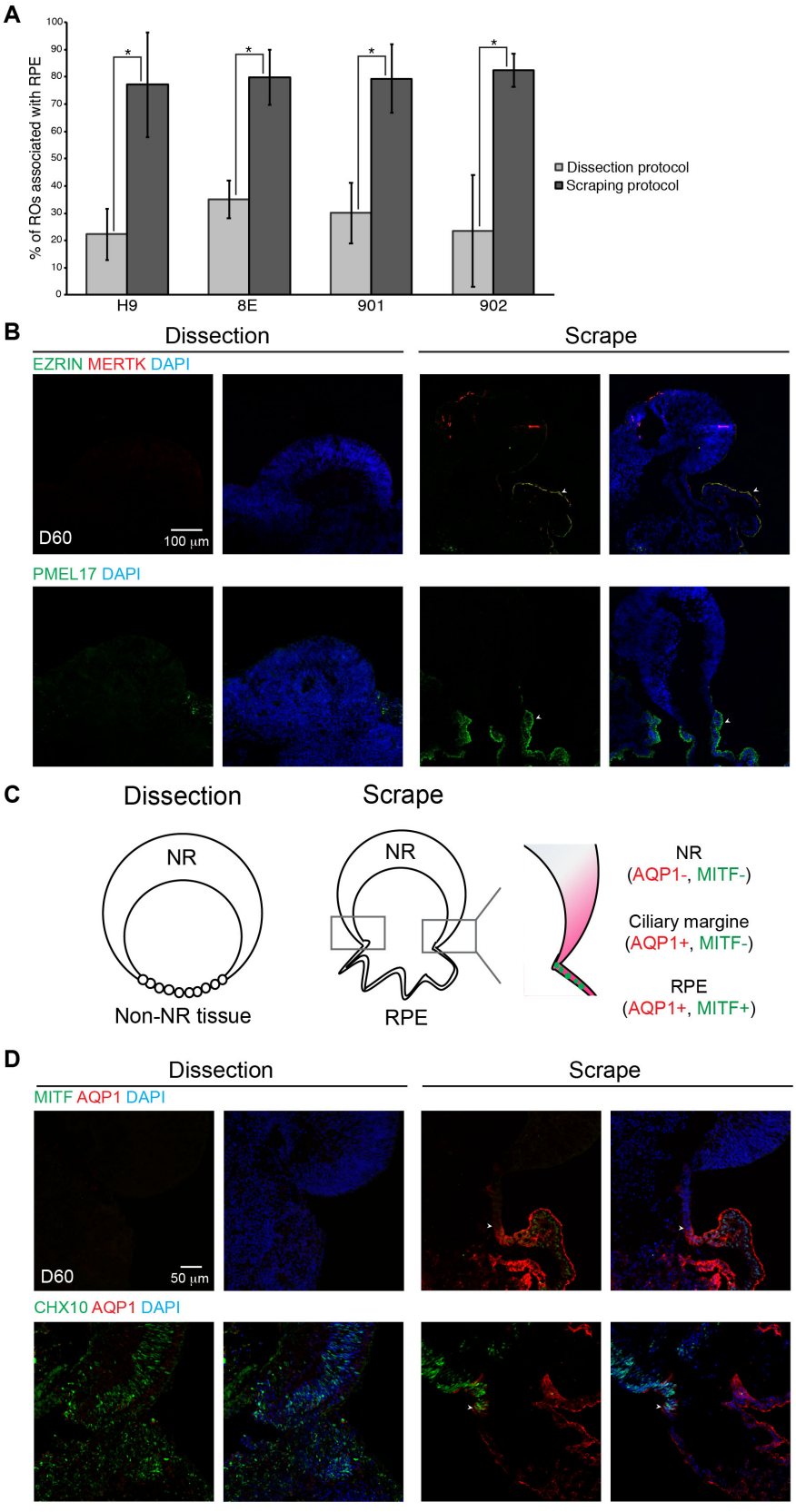

Figure 3. Cogeneration of the neural retina and pigmented epithelium is enhanced by the scraping differentiation method. **A**: Proportion of retinal organoids (ROs) associated with pigmented epithelium domain. The bar charts summarized data from three independent experiments using four different human pluripotent stem cell (hPSC) lines and presented as mean ± standard deviation. *p<0.05. **B**: Pigmented epithelium (PE) of pigmented domain shown by EZRIN (green, upper), MERTK (red, upper), and PMEL17 (green, lower). **C**: Schematic representation of CHX10, MITF, and AQP-1 staining in ROs obtained with the dissection and scraping methods. **D**: Immunostaining of retinal progenitor cell marker CHX10, ciliary epithelium marker AQP-1, and PE marker MITF. Nuclei were stained with 4′,6-diamidino-2-phenylindole (DAPI, blue). Arrowheads indicate relevant staining of each marker.

DISCUSSION

We described a modified differentiation protocol for efficient production of ROs from hPSCs. Replacement of the dissection step with a simpler and less labor-intensive scraping method not only saves time but also increases the yield of RO production by up to about fivefold. Moreover, as the whole adherent culture is scraped off, this method circumvents subjective selection of OVs-like domains which, when adherent to plastic dishes, do not always display a readily identifiable morphology. These features make the new method far more robust and accessible to inexperienced personnel. With this new method, we consistently obtained ROs from cultures depleted of all apparent OVs-like domains by dissection, which indicates that organoids emerged from areas without typical morphology and explains the higher yield of the scraping method. Whether these ROs emerged from specified retinal progenitors that failed to form typical OV-like structures in adherent culture conditions, or from less mature eye field progenitors whose differentiation could be stimulated by the 2D to 3D transition remains to be determined. Regardless, this observation suggests the prevalence of latent OVs or eye field cells that are constrained in adherent cultures but are released from such inhibition upon transitioning to 3D conditions. This idea can be best understood in the context of matrix stiffness and mechanical forces having a profound influence on stem cell development [23]. OVs in vivo evaginate from the anterior neural plate where tissue stiffness is measured in dozens of Pascals in contrast to the standard in vitro culture dish measured in millions of Pascals, differing in stiffness by orders of magnitude. The hypothesis that a softer matrix environment favors eye field specification and OV generation remains to be validated experimentally.

We have shown that organoids obtained with this new scraping method displayed morphology similar to that of the dissected organoids and recapitulated the temporal development of the in vivo retina [24], with initial biogenesis of early-born retinal cell types, such as RGCs and horizontal cells, followed by specification of bipolar and Müller cells concomitantly with photoreceptor maturation. Importantly, no differentiation delay or increased variability among organoids was observed using the scraping method. Recent studies indicated that the proportion of cone and rod photoreceptors in ROs could be modified by modulation of key signaling pathways, such as DHA and FGF1 [25], Notch [26], retinoic acid [26], IGF-1 [27], and thyroid hormone [26,28]. Such modifications could be implemented in the new scraping method for applications requiring enrichment of a specific cell type.

Another interesting observation in this study was more frequent cogeneration of the NR and RPE using the scraping protocol. One possible explanation is that ROs are able to retain surrounding tissues by scraping, leading to the conservation of RPE precursors that may be removed by dissection. As shown in a previous study, RPE spheroids consistently emerge from the remaining adherent cells after dissection of OVs [29]. Despite the high proportion of ROs associated with RPE domains, however, we never detected direct apposition of RPE and NR as is observed in the in vivo retina after optic cup invagination, an observation consistent with previous reports [17,22]. Nevertheless, we noted the presence of a distinct pool of cells at the NR and RPE junction(s), with the expression of ciliary epithelium marker AQP1 but not RPE marker MITF. This pool of cells could represent the ciliary margin stem cells described in a previous study [22], in which a complex “induction-reversal method” was used to manipulate cell fate specification and promote cogeneration of the RPE and NR. However, although the method presented here is simpler, additional investigations are required to confirm “stemness” and the proliferative capacity of this particular domain.

Despite the improved yields, photoreceptors in the organoid cultures in this study still lacked outer segment structures with well-stacked discs. Comparative transcriptome analyses of human adult retina and hPSC-derived organoids revealed downregulation of many phototransduction genes in cultures [11], suggesting that retinal organoids are not yet functionally mature. Given the crucial role of RPE in photoreceptor outer segment homeostasis [30], it has long been postulated that coculture of ROs in direct apposition with RPE could improve photoreceptor maturation. The recently reported retina-on-a-chip model, which incorporates the coculture of RPE and ROs in a microfluidic system, enhanced the formation of outer segment–like structures [31], although the photoreceptor outer segments in these organoids still lacked organized discs. An alternative approach used decellularized extracellular matrix–derived peptides from the bovine NR and RPE, which may enhance synaptogenesis and light responsiveness of human ROs [32]. Improvement of oxygenation and material exchanges, by culturing organoids in a rotating bioreactor, also increased the yield of photoreceptors [33,34], suggesting a crucial role of the microenvironment in organoid differentiation. Additional investigations are necessary to identify and incorporate additional missing factors for photoreceptor maturation in vitro.

To conclude, by increasing the yield while decreasing the complexity of RO production, the method described in this study should facilitate the development of applications

requiring large-scale generation of ROs, such as high-throughput drug screening, and benefit less experienced researchers in their quest for a simple and reliable method for generating ROs. Consequently, this method presents a valuable in vitro platform for understanding retinal development and evaluating effective treatments for diseases.

APPENDIX 1. ANTIBODY INFORMATION FOR IMMUNOSTAINING.

To access the data, click or select the words "Appendix 1."

ACKNOWLEDGMENTS

We thank Drs. Kamil Kruczek and Charlie Drinnan for helpful discussions. This research was supported by Intramural Research Program of the National Eye Institute (ZIAEY000490, ZIAEY000474, ZIA000546), and Mr. Yair Mendels through the USHER2020 Foundation.

REFERENCES

1. Scholl HP, Strauss RW, Singh MS, Dalkara D, Roska B, Picaud S, Sahel JA. Emerging therapies for inherited retinal degeneration. Sci Transl Med 2016; 8:368rv6-[PMID: 27928030].
2. Duncan JL, Pierce EA, Laster AM, Daiger SP, Birch DG, Ash JD, Iannaccone A, Flannery JG, Sahel JA, Zack DJ, Zarbin MA. and the Foundation Fighting Blindness Scientific Advisory B. Inherited Retinal Degenerations: Current Landscape and Knowledge GapsTransl Vis Sci Technol 2018; 7:6-[PMID: 30034950].
3. Eiraku M, Takata N, Ishibashi H, Kawada M, Sakakura E, Okuda S, Sekiguchi K, Adachi T, Sasai Y. Self-organizing optic-cup morphogenesis in three-dimensional culture. Nature 2011; 472:51-6. [PMID: 21475194].
4. Nakano T, Ando S, Takata N, Kawada M, Muguruma K, Sekiguchi K, Saito K, Yonemura S, Eiraku M, Sasai Y. Self-formation of optic cups and storable stratified neural retina from human ESCs. Cell Stem Cell 2012; 10:771-85. [PMID: 22704518].
5. Sasai Y, Eiraku M, Suga H. In vitro organogenesis in three dimensions: self-organising stem cells. Development 2012; 139:4111-21. [PMID: 23093423].
6. Meyer JS, Howden SE, Wallace KA, Verhoeven AD, Wright LS, Capowski EE, Pinilla I, Martin JM, Tian S, Stewart R, Pattnaik B, Thomson JA, Gamm DM. Optic vesicle-like structures derived from human pluripotent stem cells facilitate a customized approach to retinal disease treatment. Stem Cells 2011; 29:1206-18. [PMID: 21678528].
7. Zhong X, Gutierrez C, Xue T, Hampton C, Vergara MN, Cao LH, Peters A, Park TS, Zambidis ET, Meyer JS, Gamm DM, Yau KW, Canto-Soler MV. Generation of three-dimensional retinal tissue with functional photoreceptors from human iPSCs. Nat Commun 2014; 5:4047-[PMID: 24915161].
8. Reichman S, Slembrouck A, Gagliardi G, Chaffiol A, Terray A, Nanteau C, Potey A, Belle M, Rabesandratana O, Duebel J, Orieux G, Nandrot EF, Sahel JA, Goureau O. Generation of Storable Retinal Organoids and Retinal Pigmented Epithelium from Adherent Human iPS Cells in Xeno-Free and Feeder-Free Conditions. Stem Cells 2017; 35:1176-88. [PMID: 28220575].
9. Wahlin KJ, Maruotti JA, Sripathi SR, Ball J, Angueyra JM, Kim C, Grebe R, Li W, Jones BW, Zack DJ. Photoreceptor Outer Segment-like Structures in Long-Term 3D Retinas from Human Pluripotent Stem Cells. Sci Rep 2017; 7:766-[PMID: 28396597].
10. Hallam D, Hilgen G, Dorgau B, Zhu L, Yu M, Bojic S, Hewitt P, Schmitt M, Uteng M, Kustermann S, Steel D, Nicholds M, Thomas R, Treumann A, Porter A, Sernagor E, Armstrong L, Lako M. Human-Induced Pluripotent Stem Cells Generate Light Responsive Retinal Organoids with Variable and Nutrient-Dependent Efficiency. Stem Cells 2018; 36:1535-51. [PMID: 30004612].
11. Kaya KD, Chen H, Brooks M, Kelley R, Shimada H, Nagashima K, de Val N, Drinnan C, Gieser L, Kruczek K, Erceg S, Li T, Lukovic D, Adlakha Y, Welby E, Swaroop A. Transcriptome-based molecular staging of human stem cell-derived retinal organoids uncovers accelerated photoreceptor differentiation by 9-cis retinal. MolVis 2019; 25: 663-78[PMID: 31814692].
12. Kaewkhaw R, Swaroop M, Homma K, Nakamura J, Brooks M, Kaya KD, Chaitankar V, Michael S, Tawa G, Zou J, Rao M, Zheng W, Cogliati T, Swaroop A. Treatment Paradigms for Retinal and Macular Diseases Using 3-D Retina Cultures Derived From Human Reporter Pluripotent Stem Cell Lines. nvest Ophthalmol Vis Sci. 2016 Apr; 57(5): ORSFl1–ORSFl11.
13. Shimada H, Lu Q, Insinna-Kettenhofen C, Nagashima K, English MA, Semler EM, Mahgerefteh J, Cideciyan AV, Li T, Brooks BP, Gunay-Aygun M, Jacobson SG, Cogliati T, Westlake CJ, Swaroop A. In Vitro Modeling Using Ciliopathy-Patient-Derived Cells Reveals Distinct Cilia Dysfunctions Caused by CEP290 Mutations. Cell Reports 2017; 20:384-96. [PMID: 28700940].
14. Jin ZB, Okamoto S, Osakada F, Homma K, Assawachananont J, Hirami Y, Iwata T, Takahashi M. Modeling retinal degeneration using patient-specific induced pluripotent stem cells. PLoS One 2011; 6:e17084-[PMID: 21347327].
15. Deng WL, Gao ML, Lei XL, Lv JN, Zhao H, He KW, Xia XX, Li LY, Chen YC, Li YP, Pan D, Xue T, Jin ZB. Gene Correction Reverses Ciliopathy and Photoreceptor Loss in iPSC-Derived Retinal Organoids from Retinitis Pigmentosa Patients. Stem Cell Reports 2018; 10:1267-81. [PMID: 29526738].
16. Parfitt DA, Lane A, Ramsden CM, Carr AJ, Munro PM, Jovanovic K, Schwarz N, Kanuga N, Muthiah MN, Hull S, Gallo JM, da Cruz L, Moore AT, Hardcastle AJ, Coffey PJ, Cheetham ME. Identification and Correction of Mechanisms Underlying Inherited Blindness in Human iPSC-Derived

Optic Cups. Cell Stem Cell 2016; 18:769-81. [PMID: 27151457].

17. Capowski EE, Samimi K, Mayerl SJ, Phillips MJ, Pinilla I, Howden SE, Saha J, Jansen AD, Edwards KL, Jager LD, Barlow K, Valiauga R, Erlichman Z, Hagstrom A, Sinha D, Sluch VM, Chamling X, Zack DJ, Skala MC, Gamm DM. Reproducibility and staging of 3D human retinal organoids across multiple pluripotent stem cell lines. Development 2019; 146:dev17688[PMID: 30567931].

18. Reichman S, Terray A, Slembrouck A, Nanteau C, Orieux G, Habeler W, Nandrot EF, Sahel JA, Monville C, Goureau O. From confluent human iPS cells to self-forming neural retina and retinal pigmented epithelium. Proc Natl Acad Sci USA 2014; 111:8518-23. [PMID: 24912154].

19. Strauss O. The retinal pigment epithelium in visual function. Physiol Rev 2005; 85:845-81. [PMID: 15987797].

20. Kaewkhaw R, Kaya KD, Brooks M, Homma K, Zou J, Chaitankar V, Rao M, Swaroop A. Transcriptome Dynamics of Developing Photoreceptors in Three-Dimensional Retina Cultures Recapitulates Temporal Sequence of Human Cone and Rod Differentiation Revealing Cell Surface Markers and Gene Networks. Stem Cells 2015; 33:3504-18. [PMID: 26235913].

21. Mellough CB, Collin J, Queen R, Hilgen G, Dorgau B, Zerti D, Felemban M, White K, Sernagor E, Lako M. Systematic Comparison of Retinal Organoid Differentiation from Human Pluripotent Stem Cells Reveals Stage Specific, Cell Line, and Methodological Differences. Stem Cells Transl Med 2019; 8:694-706. [PMID: 30916455].

22. Kuwahara A, Ozone C, Nakano T, Saito K, Eiraku M, Sasai Y. Generation of a ciliary margin-like stem cell niche from self-organizing human retinal tissue. Nat Commun 2015; 6:6286-[PMID: 25695148].

23. Vining KH, Mooney DJ. Mechanical forces direct stem cell behaviour in development and regeneration. Nat Rev Mol Cell Biol 2017; 18:728-42. [PMID: 29115301].

24. Hoshino A, Ratnapriya R, Brooks MJ, Chaitankar V, Wilken MS, Zhang C, Starostik MR, Gieser L, La Torre A, Nishio M, Bates O, Walton A, Bermingham-McDonogh O, Glass IA, Wong ROL, Swaroop A, Reh TA. Molecular Anatomy of the Developing Human Retina. Dev Cell 2017; 43:763-79. e4. [PMID: 29233477].

25. Brooks MJ, Chen HY, Kelley RA, Mondal AK, Nagashima K, De Val N, Li T, Chaitankar V, Swaroop A. Improved Retinal Organoid Differentiation by Modulating Signaling Pathways Revealed by Comparative Transcriptome Analyses with Development In Vivo. Stem Cell Reports 2019; 13:891-905. [PMID: 31631019].

26. Zerti D, Dorgau B, Felemban M, Ghareeb AE, Yu M, Ding Y, Krasnogor N, Lako M. Developing a simple method to enhance the generation of cone and rod photoreceptors in pluripotent stem cell-derived retinal organoids. Stem Cells 2019; 38:45-51[PMID: 31670434].

27. Chichagova V, Hilgen G, Ghareeb A, Georgiou M, Carter M, Sernagor E, Lako M, Armstrong L. Human iPSC differentiation to retinal organoids in response to IGF1 and BMP4 activation is line- and method-dependent. Stem Cells 2019; 38:195-201[PMID: 31721366].

28. Eldred KC, Hadyniak SE, Hussey KA, Brenerman B, Zhang PW, Chamling X, Sluch VM, Welsbie DS, Hattar S, Taylor J, Wahlin K, Zack DJ, Johnston RJ Jr. Thyroid hormone signaling specifies cone subtypes in human retinal organoids. Science 2018; 362:pii: eaau6348[PMID: 30309916].

29. Liu S, Xie B, Song X, Zheng D, He L, Li G, Gao G, Peng F, Yu M, Ge J, Zhong X. Self-Formation of RPE Spheroids Facilitates Enrichment and Expansion of hiPSC-Derived RPE Generated on Retinal Organoid Induction Platform. Invest Ophthalmol Vis Sci 2018; 59:5659-69. [PMID: 30489625].

30. Nasonkin IO, Merbs SL, Lazo K, Oliver VF, Brooks M, Patel K, Enke RA, Nellissery J, Jamrich M, Le YZ, Bharti K, Fariss RN, Rachel RA, Zack DJ, Rodriguez-Boulan EJ, Swaroop A. Conditional knockdown of DNA methyltransferase 1 reveals a key role of retinal pigment epithelium integrity in photoreceptor outer segment morphogenesis. Development 2013; 140:1330-41. [PMID: 23406904].

31. Achberger K, Probst C, Haderspeck J, Bolz S, Rogal J, Chuchuy J, Nikolova M, Cora V, Antkowiak L, Haq W, Shen N, Schenke-Layland K, Ueffing M, Liebau S, Loskill P. Merging organoid and organ-on-a-chip technology to generate complex multi-layer tissue models in a human retina-on-a-chip platform. eLife 2019; 8:e46188-[PMID: 31451149].

32. Dorgau B, Felemban M, Hilgen G, Kiening M, Zerti D, Hunt NC, Doherty M, Whitfield P, Hallam D, White K, Ding Y, Krasnogor N, Al-Aama J, Asfour HZ, Sernagor E, Lako M. Decellularised extracellular matrix-derived peptides from neural retina and retinal pigment epithelium enhance the expression of synaptic markers and light responsiveness of human pluripotent stem cell derived retinal organoids. Biomaterials 2019; 199:63-75. [PMID: 30738336].

33. Ovando-Roche P, West EL, Branch MJ, Sampson RD, Fernando M, Munro P, Georgiadis A, Rizzi M, Kloc M, Naeem A, Ribeiro J, Smith AJ, Gonzalez-Cordero A, Ali RR. Use of bioreactors for culturing human retinal organoids improves photoreceptor yields. Stem Cell Res Ther 2018; 9:156-[PMID: 29895313].

34. DiStefano T, Chen HY, Panebianco C, Kaya KD, Brooks MJ, Gieser L, Morgan NY, Pohida T, Swaroop A. Accelerated and Improved Differentiation of Retinal Organoids from Pluripotent Stem Cells in Rotating-Wall Vessel Bioreactors. Stem Cell Reports 2018; 10:300-13. [PMID: 29233554].

Articles are provided courtesy of Emory University and the Zhongshan Ophthalmic Center, Sun Yat-sen University, P.R. China. The print version of this article was created on 3 March 2020. This reflects all typographical corrections and errata to the article through that date. Details of any changes may be found in the online version of the article.